Multi-frequency electrical impedance tomography (EIT) of the adult human head: initial findings in brain tumours, arteriovenous malformations and chronic stroke, development of an analysis method and calibration

A Romsauerova[1], A McEwan[1], L Horesh[1], R Yerworth[1], R H Bayford[2] and D S Holder[1]

[1] Department of Medical Physics and Bioengineering, UCL, London, UK
[2] School of Health, Environment and Biological Sciences, Middlesex University, Archway Campus, London, N19 5ND, UK

E-mail: a.romsauerova@ucl.ac.uk

Abstract

MFEIT (multi-frequency electrical impedance tomography) could distinguish between ischaemic and haemorrhagic stroke and permit the urgent use of thrombolytic drugs in patients with ischaemic stroke. The purpose of this study was to characterize the UCLH Mk 2 MFEIT system, designed for this purpose, with 32 electrodes and a multiplexed 2 kHz to 1.6 MHz single impedance measuring circuit. Data were collected in seven subjects with brain tumours, arteriovenous malformations or chronic stroke, as these resembled the changes in haemorrhagic or ischaemic stroke. Calibration studies indicated that the reliable bandwidth was only 16–64 kHz because of front-end components placed to permit simultaneous EEG recording. In raw in-phase component data, the SD of 16–64 kHz data for one electrode combination across subjects was $2.45 \pm 0.9\%$, compared to a largest predicted change of 0.35% estimated using the FEM of the head. Using newly developed methods of examining the most sensitive channels from the FEM, and nonlinear imaging constrained to the known site of the lesion, no reproducible changes between pathologies were observed. This study has identified a specification for accuracy in EITS in acute stroke, identified the size of variability in relation to this in human recordings, and presents new methods for analysis of data. Although no reproducible

changes were identified, we hope this will provide a foundation for future studies in this demanding but potentially powerful novel application.

1. Introduction

1.1. Potential use of EIT for providing urgent neuroimaging in acute stroke to permit the use of thrombolytic therapy

The possible use of MFEIT for rapid neuroimaging in acute stroke is very attractive, as it could be used in casualty or the community to distinguish haemorrhagic from ischaemic stroke and so permit the use of thrombolytic (clot-dissolving) drugs. Until recently, there has been no treatment for acute stroke—the pathology is left to evolve without intervention. In the past decade, it has been shown that administration of a thrombolytic agent, such as tPa, substantially reduces morbidity and mortality (Osborn *et al* 1999). However, this has not been widely taken up; because it has to be given very rapidly, otherwise the ischaemic brain becomes irretrievably damaged. In practice, this is within 3–6 h. In addition, urgent neuroimaging must be performed first, as the clinical appearances of a stroke are identical but can be due to ischaemic stroke, due to occlusion of an artery, but also a haemorrhage. Thrombolytic therapy must not be given in the latter case, as the haemorrhage may extend. The non-contrast head CT scan remains the first-line imaging study in suspected stroke patients due to its exquisite sensitivity for the detection of blood (Hankey and Warlow 1999). In practice, it is impossible to obtain an urgent CT and have it reported in the time available, except for dedicated highly equipped centres. EIT is portable and inexpensive. In principle, it could provide urgent neuroimaging in such an acute situation—a scan could be collected in a few minutes with the use of a headnet, and it could be rapidly reported over the internet by a radiologist.

1.2. Background

1.2.1. Physiological basis for expecting bioimpedance changes in stroke and related conditions. The magnitude of the expected changes may be estimated from values of the impedance in the literature and the expected dilution of these when measured on the scalp. The impedance of normal grey matter in the brain is due to the conductive ionic extra- and intra-cellular compartments, and many fine branched neuronal processes which give a fairly high permittivity, so that there is a substantial change of conductivity with frequency as more current passes through the cell membranes into the intracellular space (Gabriel *et al* 1996b). In contrast, blood behaves almost as an aqueous ionic solution up to over 1 MHz and so has a very flat frequency response (Gabriel *et al* 1996b). In ischaemic grey matter in the brain, extracellular water moves into the intracellular space. As a result, the low frequency conductivity is reduced, but the properties are similar at higher frequencies approaching 1 MHz; the net effect is that the change with frequency is marginally greater than normal grey matter above 100 Hz or so (Gabriel *et al* 1996b). There are therefore large differences in conductivity over frequency between blood, normal, and ischaemic brain which could be exploited by MFEIT (figure 1). Similar changes may be expected to occur in other pathology in
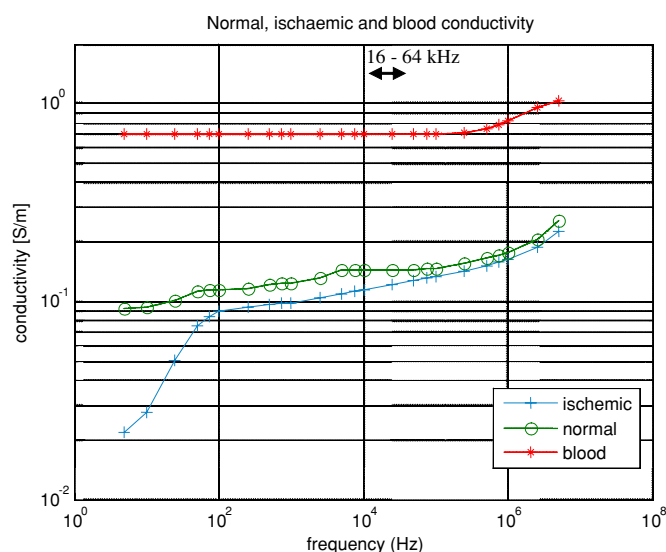
Figure 1. Conductivities for normal and ischaemic tissues in the head; compilation from a literature review (Horesh *et al* 2005a).

the brain, which resemble these—there is an increase in blood in arteriovenous malformation, malignant brain tumours are more vascular and have a larger extracellular space, and, in chronic stroke, brain tissue has been replaced by highly conductive cerebrospinal fluid.

1.2.2. Introduction to the UCLH Mk 2 multi-frequency EIT system. In our group at UCL, we have been developing the UCLH Mk 2 MFEIT system for this purpose (Yerworth *et al* 2003). Its principle was that it utilized a single impedance measuring module derived from the Sheffield Mk 3.5 MFEIT system (Wilson *et al* 2001). Unlike this system, which used parallel modules, each capable of driving current or receiving, it utilized a multiplexer which enabled it to address up to 64 electrodes. Although this was a compromise in that this introduced additional stray capacitance, it had the advantage that a larger number of electrodes could be flexibly addressed to permit evaluation of different electrode combinations. The underlying module delivers 293 μA rms over 30 frequencies from 2 kHz to 1.6 MHz.

However, various compromises had to be made in its design. In order to meet with the requirements of IEC601, additional dc blocking capacitors were introduced in each electrode line for patient safety. To allow simultaneous acquisition of EEG, resistors to ground were also introduced in each electrode to attenuate switching artefacts in the EEG band. These modifications attenuated frequencies of 4 kHz and below. In addition, capacitance in long, unscreened leads and contact impedance set the high frequency limit to 128 kHz (figure 2).

1.3. Purpose

The purpose of this study was to characterize the UCLH Mk 2 system and determine if it has sufficient accuracy to proceed to human studies in acute stroke. The goals of this work were (1) to determine the variability of changes in the bandwidth from which changes could reliably be recorded, (2) to develop methods short of full image reconstruction to attempt to discriminate small changes which may have been statistically significant but may not have shown up in images, (3) to determine any shortcomings in instrumentation, and (4) to ascertain
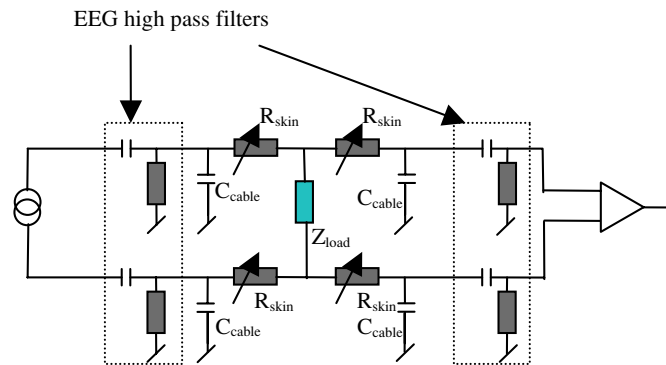
EEG high pass filters

Figure 2. Circuit diagram of filters at each electrode of the Mk 2 UCLH system. R_{skin} is typically 1 kΩ. C_{cable} was approximately 50 pF for 1 m long cables. The EEG high pass filters consisted of 0.01 μF dc-blocking capacitors and 10 kΩ resistor to ground.

if any significant differences could indeed be observed between pathology and normal brain in human subjects.

1.4. Experimental design

In order to discriminate these pathologies, it was essential that the system had a flat frequency response and that this was independent of the load measured. This was tested by recording the raw impedance data from a cylindrical tank with 16 electrodes while saline solution was serially diluted to give equivalent loads to those encountered in the adult human head.

Human measurements were then made in subjects with conditions that could conveniently be recorded in an out-patient setting, but which resembled the changes in haemorrhagic or ischaemic stroke—brain tumours, arteriovenous malformations (AVMs) or chronic stroke, in which the resorbed infarcted brain is occupied by cerebrospinal fluid, which resembles blood.

Data were initially processed by reconstruction of EIT images of abnormalities using a linear frequency difference method. In the event, it was not possible to obtain reproducible images of the known pathology in the subjects. We therefore developed alternative methods with the intention that they might reveal significant changes even though these might not be apparent in reconstructed images. (1) We used an accurate anatomical finite element model of the head to estimate which electrode combinations were most sensitive to each subject's pathology, based on their MRI. The boundary voltage in the 25% of the most sensitive channels was compared for the pathological region and a normal mirror region from the contralateral side of the brain on the image. (2) Images of absolute conductivity were reconstructed with a nonlinear iterative method. Conductivity at different frequencies was constrained to the whole brain compartment and the known region of the pathology. Although, this would clearly not be useful in the intended clinical situation in acute stroke, as the region of pathology would not be known, it was undertaken in order to increase the chances of finding a significant change. This was termed 'compartment-wise reconstruction'.

1.5. Expected impedance changes

1.5.1. Expected local impedance changes in the brain in acute stroke or haemorrhage. The expected changes locally in the brain during acute stroke or haemorrhage ranged from 0.2% to 185% depending on the frequency range and condition (table 1).

Table 1. Expected conductivity frequency differences if recorded locally in the brain (Horesh *et al* 2005c)

Frequency range	Blood (%)	Ischaemic grey matter (%)	Normal grey matter (%)
16–64 kHz	0.2	12	1
4–128 kHz	0.5	25	12
20 Hz to 1 MHz	18	185	75

Table 2. Boundary voltages for maximal absolute change channel restricted to diametrically opposed injection and adjacent measurement.

	16 kHz (mV)	64 kHz (mV)	Diff (μV) (64–16 kHz)	Diff (%)
Normal	1.780	1.753	–26.3	–1.491
Large Haemorrhage	1.634	1.614	–20.3	–1.247

1.5.2. Expected local changes in the brain during AVM, tumours or chronic stroke.   Changes in an AVM or chronic stroke, in which necrotic brain tissue is replaced by cerebrospinal fluid, would resemble blood, and those in a tumour, ischaemic brain (Cone and Cone 1976, Pethig 1987, Surowiec *et al* 1988, Haemmerich *et al* 2003).

1.5.3. Limitations in bandwidth available for recording with the UCLH Mk 2 EIT system. Ideally, measurement should be in the range from 20 Hz to 1.6 MHz, where the largest frequency difference changes are expected to occur, but tank calibration indicated that, for the UCLH Mk 2, only 4–128 kHz appeared to be reliable. Unfortunately, although the system worked satisfactorily in the range 4–128 kHz in the tank, in human studies, there was an unexpected roll-off at extremes; analysis in human data was therefore undertaken by comparing the in-phase measurement in the restricted range of 16–64 kHz. The expected changes can be determined by reference to published impedance properties in the literature, which are summarized in figure 2. In this range of 16–64 kHz, blood, normal, and ischaemic brain decrease resistivity by about 0.2%, 1% and 12%, respectively (figure 1, table 1).

1.5.4. Expected size of changes when recorded on the scalp.   Impedance changes which occur locally in the brain will be substantially reduced in size when recorded with scalp electrodes, because of partial volume effects and the blurring effect of the skull and extracerebral layers. These effects have been modelled in our group, using a fine realistic FEM of the head. Gilad *et al* (2005) considered time difference changes in dc conductivity due to neuronal activity in the visual cortex (a centrally-located, plum-sized area of the brain). They found that the most sensitive channels on the surface detected changes two to three orders of magnitude smaller than the local changes.

The standing boundary voltage differences between 64 and 16 kHz have been estimated using a detailed FEM of the head, in which impedance properties of the brain, CSF, skull and scalp were inserted from the literature (Horesh *et al* 2005c) (table 2). A detailed analysis is outside the scope of this paper, but an example may serve to give an upper bound for required accuracy. For a haemorrhage, 47.7 ml in volume, near the edge of skull, in the most
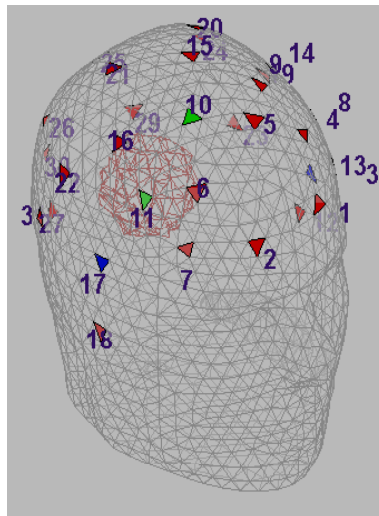
Figure 3. Example of conductivity change for haemorrhagic lesion, 47.7 ml in volume, near the scalp. The largest change was estimated to be with diametrically opposed current injection (through electrodes 13 and 17) and adjacent measurement (through electrodes 10 and 11).

sensitive channel, the standing potential is about 2 mV and the difference in recorded voltage between 16 and 64 kHz is 6 μV, or about 0.35% of the standing potential. Changes larger than 50% of this were estimated to occur in 7% of electrode combinations (figure 3). The change for tumours may be expected to be about ten times larger—i.e. of the order of 3%. In estimating a desired accuracy for the instrumentation, other factors need to be taken into account: this estimate was for a large lesion near the edge of the brain, in the study, some lesions were smaller and deeper; for reliable stroke type detection, it may not be sufficient to record changes just in 10% of electrodes; to detect changes, the instrumentation should have an accuracy perhaps ten times greater than the change being recorded. Taking all these factors into account, and that the largest change in this frequency range was between tumour and haemorrhage at 12%, an upper bound for instrumentation accuracy might reasonably be set at 0.1% over the frequency range. In other words, the frequency difference in-phase recording between 16 kHz and 64 kHz should be accurate to more than 0.1% of the load measured at one of the frequencies.

2. Methods

2.1. Saline dilution studies

A saline filled 2D cylindrical tank, 10 cm diameter and 8 cm high, with 16 stainless steel electrodes in a ring, was filled with 0.2% saline, which was serially diluted in steps of 10% (figure 4). Using a diametric protocol, 100 sets of 96 boundary voltages were collected for each dilution, with the UCLH Mk 2. Data were collected over 2 kHz to 1.6 MHz with an applied rms current of 293 μA. The system was calibrated using corrections for phase and gain recorded on one channel with a resistor of 20 Ω; this was applied equally to all electrode combinations.

Data were also collected from a saline filled head-shaped 3D tank using a modified 10–20 EEG electrode placement scheme. (Tidswell *et al* 2001). The system was calibrated
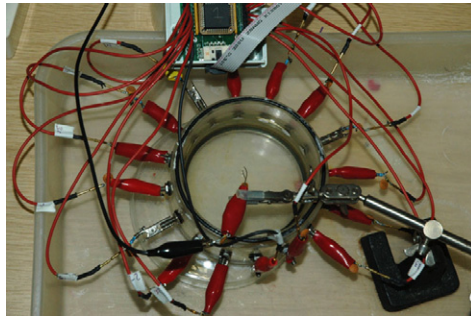
Figure 4. Saline filled cylindrical tank.

using corrections for phase and gain according to the mean of all 96 electrode combinations recorded in the 2D tank filled with 0.2% saline; this was applied equally to all electrode combinations.

2.2. Human data collection

Data were recorded with the UCLH Mk 2 EIT system in seven patients with chronic stroke, brain tumours, or AVMs, with lesion sizes from 1.5 to 7 cm in diameter (the appendix). 31 EEG electrodes were placed on the head after skin abrasion using a modified 10–20 EEG electrode placement scheme. (Tidswell *et al* 2001) (figure 5). The contact impedance was checked using two terminal impedance measurements between electrode 1 and the other 31 electrodes. Each image data set comprised 258 impedance measurements made from combinations of the 31 EEG electrodes attached by unscreened leads up to 1 m long. Each patient gave informed consent. The Joint UCL/UCLH Committees on the Ethics of Human Research approved this study. Ten images were collected from each patient using a current waveform over 2 kHz to 1.6 MHz and a current of 293 μA RMS. The system was calibrated using corrections for phase and gain according to the mean of all 258 electrode combinations recorded in the 3D tank filled with 0.2% saline; this was applied equally to all electrode combinations.
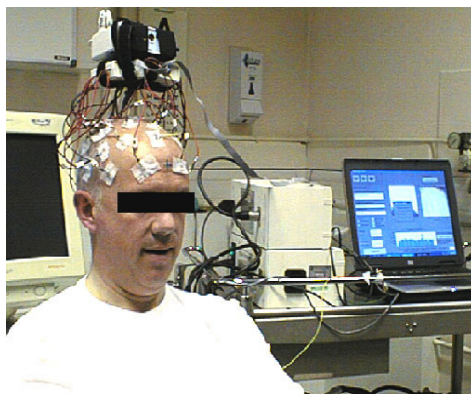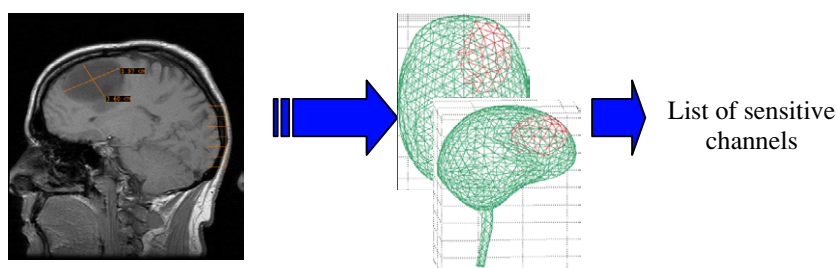

Figure 5. Patient data collection.

Figure 6. Example of a brain tumour, segmented and inserted into the FEM, and used to calculate the most sensitive channels.

2.3. Analysis of between patient variation

Data were processed after adjustment according to the calibration data of phase and gain determined using the 3D head shaped tank. The Mk 2 EITS system has fixed gain; as a result, up to 50 channels in each subject saturated in human recordings and were discarded. The ratio of the in-phase component at 64 kHz divided by that at 16 kHz were analysed for between patient variation. This was undertaken by calculating the SD of the change across the seven subjects for one electrode combination. The mean and SD of these SDs across all 258 electrode combinations are then presented.

2.4. Sensitive channel analysis

An anatomically realistic Finite Element mesh of the head, with 31 111 elements (Tizzard *et al* 2005) and lesion location from individual patient MRIs, was used to calculate the relative sensitivity of each EIT electrode combination to the lesion and relevant boundary voltages (figure 6). Scalp 64/16 kHz resistance ratios for the 25% of channels that were most sensitive to each lesion, and those most sensitive to the contralateral side of the head without the lesion, for comparison, were compared using two way ANOVA.

2.5. Image reconstruction

2.5.1. Linear frequency difference reconstruction. Reconstruction of the frequency difference images (64/16 kHz) of measurements made by Mark 2 was performed by using the tSVD₋ linear reconstruction algorithm, which had a sensitivity matrix based on a forward model of a head-shaped model of the head (Tidswell *et al* 2001). The same idealized model and electrode positions were used to reconstruct all images. Truncated singular value decomposition (tSVD) was used to invert the sensitivity matrix with a truncation of 50 singular values.

2.5.2. Compartment-wise reconstruction. A five-shell finite element model, comprising five regions of scalp, skull, CSF layers, grey and white matter was used respectively (Horesh *et al* 2005c). The known shape of the lesion derived from MRI and its contralateral mirror side were segmented in the forward model mesh. Each of the regions together with the lesion and the mirrored lesion were noted as compartments, and the lesions were assigned with the initial impedance values of their surrounding region. Initial impedance values were obtained from the literature for the MK2 EIT system frequency range (2 kHz to 1.6 MHz) (Ranck Jr 1963a, 1963b, Ranck 1964, Ranck Jr and BeMent 1965), (Gabriel *et al* 1996a, 1996b, 1996c). Electrodes were positioned according to the extended 10–20 EEG scheme, which provided
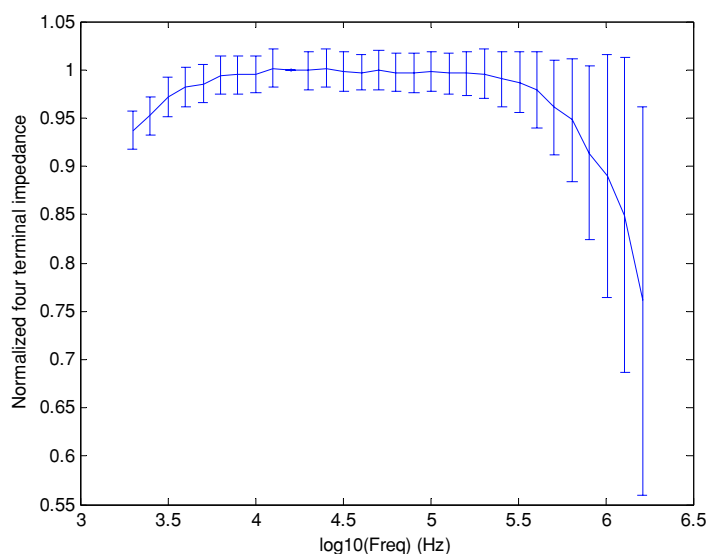
Figure 7. Calibration curve (mean and ±1 SD of 258 electrode combinations) from the 3D skull-shaped tank with 0.2% saline normalized to 16 kHz.

uniform sampling of the scalp area. A compartment-wise sensitivity matrix was generated from the current field and adjacent measurement field solutions and a nonlinear inverse method (Levenberg–Marquardt) (Levenberg 1944, Marquardt 1963, Horesh *et al* 2005b) was applied over the compartments, which reduced the underdetermined and ill-posed nature of the inverse problem. Every third frequency was considered as in the UCLH Mk 2 system the frequencies are applied in 3 batches of 10.

All data are presented as mean ±1 SD.

3. Results

3.1. Saline dilution studies

The EIT system was linear with respect to the load of saline dilution, to <1 Ω error, but the gain was reduced at high and low frequencies, being –1 dB at 2 and 400 kHz relative to 16 kHz. A frequency-dependent phase shift of up to 360° was present. After phase and gain correction, and normalization to 16 kHz, the variation across all channels and all frequencies was <2%, from 4 kHz to 128 kHz, for both the cylindrical and head-shaped tanks.

3.2. Contact impedance check

The two terminal impedance between electrode 1 and each other electrode for all subjects was less than 3 kΩ at 2 kHz. The mean of two terminal impedance at 2 kHz was 1.4 kΩ which varied by between 26% and 36% between the 31 electrodes (table 3).

3.3. Human data collection

After gain and phase correction based on the tank studies, the frequency spectra across different electrode combinations in the human data varied by more than 2% below 16 kHz and above
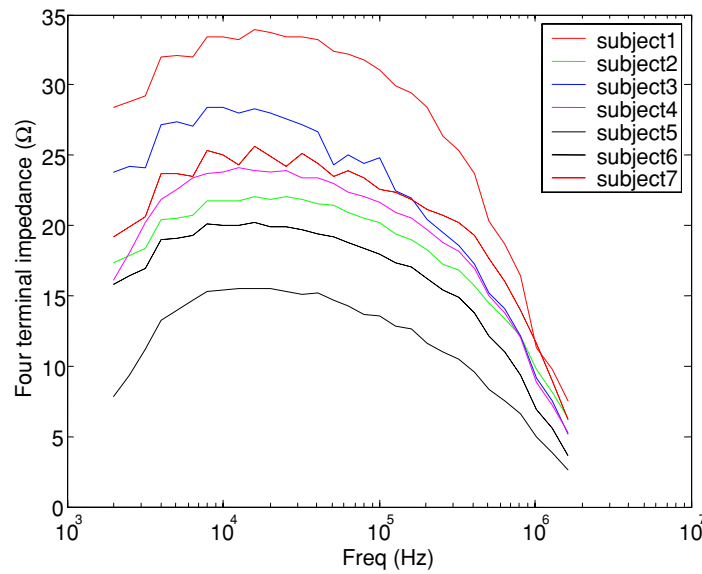
Figure 8. Impedance spectra of the 1st electrode combination of each subject after calibration.

Table 3. Two terminal impedance variation of each subject at 2 kHz.

	Max (kΩ)	Min (kΩ)	Diff (%)	Mean (kΩ)
Subject 1	1.9	1.2	35	1.5
Subject 2	1.6	1.1	30	1.2
Subject 3	1.5	1.0	30	1.2
Subject 4	1.9	1.4	26	1.7
Subject 5	2.9	1.8	36	2.2
Subject 6	2.1	1.5	30	1.8
Subject 7	1.3	0.9	32	1.0

64 kHz (figure 8). The 64/16 kHz boundary voltage ratios, averaged across all electrode combinations for all subjects, were $-6.3 \pm 2.5\%$. The variability of the 64/16 kHz frequency difference across subjects was $2.45 \pm 0.9\%$ SD.

3.4. Sensitive channel analysis

There was no significant difference between the lesion and its mirror region over all subjects, but one subject (AVM1), with the largest lesion (3 cm in diameter) showed a significant difference ($p < 0.05$) (figure 9).

3.5. Image reconstruction

3.5.1. Linear frequency difference reconstruction. EIT images were analysed visually by a radiologist (AR) and experienced clinician (DSH). There were no reproducible or recognizable changes in EIT images when compared to the known pathologies on MRI.
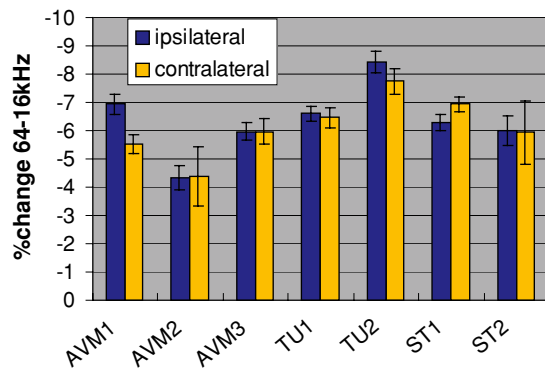
Figure 9. Resistance change between 64 kHz and 16 kHz for the lesion ('ipsilateral') and mirror area ('contralateral') (mean ± 1 SE).
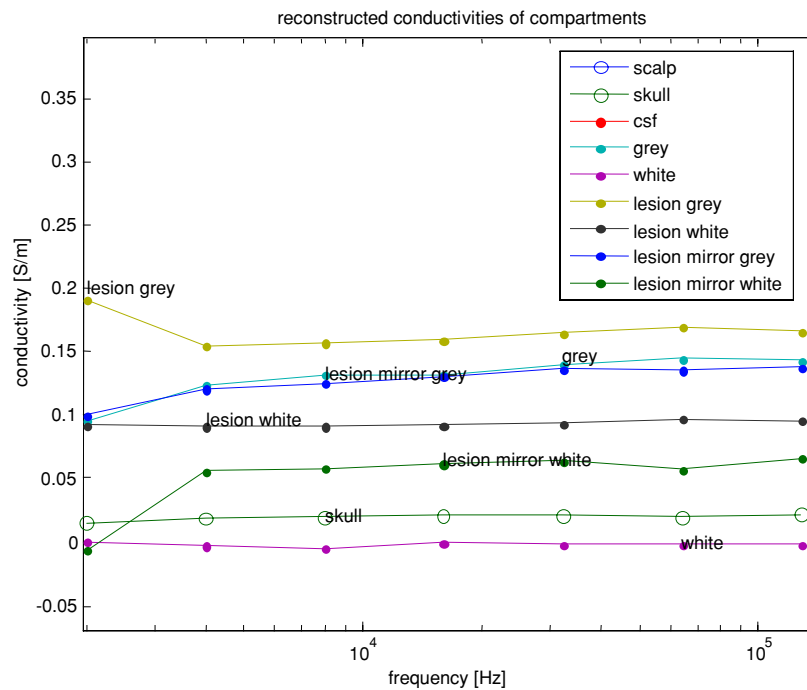

Figure 10. Patient 7 compartment-wise reconstruction of conductivity over frequency—zoomed view, CSF (cerebro-spinal fluid) and scalp properties are not displayed, due to much higher conductivity than the rest of the compartments.

3.5.2. Compartment-wise reconstruction. There were no significant differences between the lesion region with respect to the background grey matter and the mirror lesion (figure 10). In one subject, with a 7 cm diameter low grade glioma, TU2, the lesion grey matter was less resistive than the contralateral grey matter at all recorded frequencies.

4. Discussion

4.1. Summary of results

Overall, it was unfortunately not possible to observe any reproducible changes in raw data, sensitive channels or images between the three patient groups. This could be attributed to the variation in measurements over the frequency band used. The standard deviation of the in-phase component of the impedance at 64 compared to 16 kHz for the same electrode combination across subjects was about 2.5%, whereas the estimated accuracy needed was 0.1% or less.

4.2. Instrumentation considerations

Some restriction in bandwidth was predicted from the circuitry, and was observed as expected in the saline tank measurements. In addition, there was a further restriction due to the skin-electrode contact impedance in human measurements. The additional roll-off at low frequencies appears to be due to the high series skin-electrode impedance, so current was shunted to ground across the 10 kΩ resistor. The additional roll-off at high frequencies appears to be due to the combination of a lower skin-electrode impedance and stray capacitance to ground. The increased contact impedance and dc blocking capacitors may be modelled to increase the attenuation of the high pass filter, using the known values of the blocking capacitor, cable capacitance of 50 pF, and the largest recorded contact impedance of 3 kΩ. In the model, this was estimated to attenuate the EIT signals by more than 0.2 dB at 4 kHz and 16 kHz.

In principle, if the roll-off at low and high frequencies had been predictable, the effect could have been calibrated out. Unfortunately, it varies between electrode combinations (figure 7), presumably because of variations in both skin-electrode impedance of over 30% (table 2) and stray capacitance. As a result, in order to preserve accuracy independent of load over frequency, we had to restrict the reliable bandwidth to 16–64 kHz.

4.3. Possible explanation for negative finding

In order to discriminate changes between pathologies, accuracy over load and frequency of about 0.1% appears to have been needed. In the event, variability was about 2%, which is more than one order of magnitude greater. The largest expected change in the brain, between tumours and AVMs, was 12%. Although clinical studies with EIT have mainly been into the larger changes that occur with respiration or gastric emptying, smaller changes of less than this can be imaged in tanks (Holder and Khan 1994) or in imaging blood flow in the chest (Adler *et al* 1998) in time difference imaging. There have been few clinical studies of MFEIT (Brown 2003) and we are not aware of any that have successfully imaged changes of discrete pathology like this, in spite of good accuracy in tanks (Kao *et al* 2003). There therefore appears to be a disparity between the contrast sensitivity for time difference and frequency difference imaging. The added requirement for MFEIT is that the system is accurate over both frequency and load; the difficulty in human recordings is that leads and skin-electrode impedance conspire to cause changes with both of these which add to cause larger variability than the changes themselves. In this work, there were special design features which constrained the recording bandwidth more than usual, but similar problems may be expected to occur with equipment such as the Sheffield Mk 3.5 (Wilson *et al* 2001) or Dartmouth system (Halter *et al* 2005) which operate over

a broader range. In this case, although larger tissue changes may be expected to occur, larger variability in accuracy may also, and so still limit the ability to image relatively small lesions.

4.4. Use of data classification and constrained imaging

A different approach is to attempt absolute imaging. For example, absolute imaging could yield a significant result for patient 7 where the lesion grey matter is twice as conductive as the equivalent error on the contra lateral (mirror) side (figure 10). But the authors are not aware of any validated series of clinical measurements with this method. In this case, great precision is needed for the reconstruction algorithm—inaccuracy in knowledge of electrode positions, the initial impedance and the internal anatomy of the numerical model used for reconstruction, are all likely to be too great for the intended goal. In this work, we therefore elected to employ frequency difference EIT, as this at least has the potential to improve some of the systematic errors due to stray capacitance which are overcome by subtraction in time difference EIT.

Because such inaccuracies in the model used for this image reconstruction could have caused poor images, we therefore present two modified methods for data 'mining', which may be useful to others in the field who are undertaking clinical MFEIT studies.
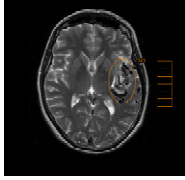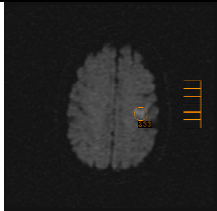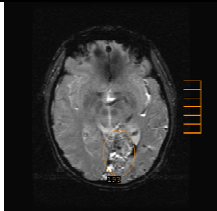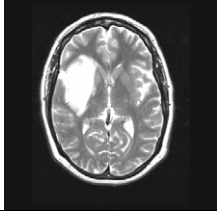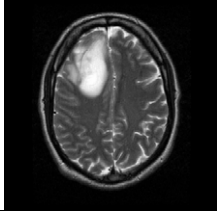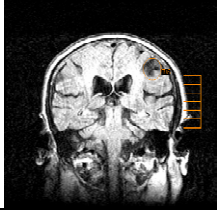
4.5. Future work

If instrumentation can be developed which can operate over the full frequency range of 20 Hz to >1 MHz, the tissue changes are large—of the order of 100% (table 1). Even with attenuation for scalp recording of two orders of magnitude, they require instrumentation accuracy of 0.1%, which appears feasible, at least on the test bench and in tank studies. For the UCLH Mk 2, we plan to remove the EEG filters to prevent the large attenuation at low frequency, minimize cable length and use driven screens to reduce capacitance to ground. Reduction of variability in electrode impedance is a priority, and it may be possible to achieve this with the use of headnets with hydrogel and improved mechanical stability (Tidswell *et al* 2003). We also plan to miniaturize the system to reduce internal stray capacitance and, in the longer term, use active electrodes and a wireless system to improve performance. The use of accurate forward models, has, for the first time, allowed us to predict the likely magnitude of the expected changes and this is likely to permit closer adjustment of instrumentation accuracy for the intended goal.

This work has provided a sound basis for future studies. With such improvements, and improved reconstruction algorithms using the same accurate head models and nonlinear methods (Horesh *et al* 2005b) with novel constraints (Haber *et al* 2004, Mayer *et al* 2005), there are still good grounds for believing that substantial advantages from using EIT to image in acute stroke may still be possible.

Appendix. MRI and details of each subject.

	Patient 1	Patient 2
Age	60	30
Diagnosis	Left temporal AVM	Right occipital AVM
MRI		
	Patient 3	Patient 4
Age	64	54
Diagnosis	Left temporal stroke	Left occipital AVM
MRI		
	Patient 5	Patient 6
Age	48	46
Diagnosis	Right temporal low grade glioma	Right frontal low grade glioma
MRI		
	Patient 7	
Age	80	
Diagnosis	Left middle frontal stroke	
MRI		

References

Adler A, Shinozuka N, Berthiaume Y, Guardo R and Bates J H 1998 Electrical impedance tomography can monitor dynamic hyperinflation in dogs *J. Appl. Physiol.* **84** 726–32

Brown B H 2003 Electrical impedance tomography (EIT): a review *J. Med. Eng. Technol.* **27** 97–108

Cone C J and Cone C 1976 Induction of mitosis in mature neurons in central nervous system by sustained depolarization *Science* **192** 155–8

Gabriel C, Gabriel S and Corthout E 1996a The dielectric properties of biological tissues: I. Literature survey *Phys. Med. Biol.* **41** 2231–49

Gabriel S, Lau R W and Gabriel C 1996b The dielectric properties of biological tissues: II. Measurements in the frequency range 10 Hz to 20 GHz *Phys. Med. Biol.* **41** 2251–69

Gabriel S, Lau R W and Gabriel C 1996c The dielectric properties of biological tissues: III. Parametric models for the dielectric spectrum of tissues *Phys. Med. Biol.* **41** 2271–93

Gilad O, Horesh L, Ahadzi G, Bayford R and Holder D 2005 Could synchronized neural activity be imaged using low frequency electrical impedance tomography (LFEIT)? *Proc. 6th Conf. on Biomedical Applications of Electrical Impedance Tomography (University College London)*

Haber E, Ascher U M and Oldenburg D W 2004 Inversion of 3D electromagnetic data in frequency and time domain using an inexact all-at-once approach *Geophysics* **69** 1216–28

Haemmerich D, Staelin D, Tsai J, Tungjitkusolmun S, Mahvi D and Webster J 2003 *In vivo* electrical conductivity of hepatic tumours *Physiol. Meas.* **24** 251–60

Halter R, Hartov A and Paulsen K D 2005 High frequency EIT for breast imaging *Proc. 6th Conf. on Biomedical Applications of Electrical Impedance Tomography (University College London)*

Hankey G and Warlow C 1999 Treatment and secondary prevention of stroke: evidence, costs, and effects on individuals and populations *Lancet* **354** 1457–63

Holder D S and Khan A 1994 Use of polyacrylamide gels in a saline-filled tank to determine the linearity of the Sheffield Mark 1 electrical impedance tomography (EIT) system in measuring impedance disturbances *Physiol. Meas.* (Suppl. 2a) **15** A45–A50

Horesh L, Gilad O, Romsauerova A, McEwan A, Arridge S R and Holder D S 2005a Stroke type differentiation by multi-frequency electrical impedance tomography—a feasibility study *EMBEC'05: 3rd Conf. on European Medical and Biological Engineering*

Horesh L, Gilad O, Romsauerova A, Tizzard A, Arridge S R and Holder D S 2005c Stroke type detection by multi-frequency electrical impedance tomography MFEIT—a feasibility study *Proc. 6th Conf. on Biomedical Applications of Electrical Impedance Tomography (University College London)*

Horesh L, Schweiger M, Arridge S R and Holder D S 2005b Large scale non-linear 3D reconstruction algorithms for electrical impedance tomography of the human brain *Conf. on Applied Inverse Problems (Royal Agricultural College, Conference Centre)*

Kao T J, Newell J C, Saulnier G J and Isaacson D 2003 Distinguishability of inhomogeneities using planar electrode arrays and different patterns of applied excitation *Physiol. Meas.* **24** 403–11

Levenberg K 1944 A method for the solution of certain problems in least squares *Q. Appl. Math.* **2** 164

Marquardt D 1963 An algorithm for least-squares estimation of nonlinear parameters *SIAM J. Appl. Math.* **11** 431

Mayer M, Brunner P, Merwa R, Smolle-Jüttner F M, Maier A and Scharfetter H 2006 Direct reconstruction of tissue parameters from differential multifrequency EIT *in vivo*, *Physiol. Meas.* **27** S93–101

Osborn T, LaMonte M and Gaasch W 1999 Intravenous thrombolytic therapy for stroke: a review of recent studies and controversies. *Ann. Emerg. Med.* **34** 244–55

Pethig R 1987 Dielectric properites of body tissue *Clin. Phys. Physiol. Meas.* **8** 5–12

Ranck J B Jr 1963a Analysis of specific impedance of rabbit cerebral cortex *Exp. Neurol.* **7** 153–74

Ranck J B Jr 1963b Specific impedance of rabbit cerebral cortex *Exp. Neurol.* **7** 144–52

Ranck J B 1964 Specific impedance of cerebral cortex during spreading depression + analysis of neuronal neuroglial + interstitial contributions *Exp. Neurol.* **9** 1–16

Ranck J B Jr and BeMent S L 1965 The specific impedance of the dorsal columns of cat: an inisotropic medium *Exp. Neurol.* **11** 451–63

Surowiec A, Stuchly S, Barr J and Swarup A 1988 Dielectric properties of breast carcinoma and the surrounding tissues *IEEE Trans. Biomed. Eng.* **35** 257–63

Tidswell A T, Bagshaw A P, Holder D S, Yerworth R J, Eadie L, Murray S, Morgan L and Bayford R H 2003 A comparison of headnet electrode arrays for electrical impedance tomography of the human head *Physiol. Meas.* **24** 527–44

Tidswell T, Gibson A, Bayford R and Holder D 2001 Three-dimensional electrical impedance tomography of human brain activity *NeuroImage* **13** 283–94

Tizzard A, Horesh L, Yerworth R, Holder D and Bayford R 2005 Generating accurate finite element meshes for the forward model of the head in EIT *Physiol. Meas.* **26** S251–S261

Wilson A J, Milnes P, Waterworth A R, Smallwood R H and Brown B H 2001 Mk 3.5: a modular, multi-frequency successor to the Mk 3a EIS/EIT system *Physiol. Meas.* **22** 49–54

Yerworth R, Bayford R, Brown B, Milnes P, Conway M and Holder D 2003 Electrical impedance tomography spectroscopy (EITS) for human head imaging *Physiol. Meas.* **24** 477–89